ARTICLE
Journal of Cellular Biochemistry 115:340–348 (2014)

Journal of Cellular Biochemistry

Effect and Possible Mechanism of Network Between MicroRNAs and *RUNX2* Gene on Human Dental Follicle Cells

Pei Chen, Dixin Wei, Baoyi Xie, Jia Ni, Dongying Xuan,* and Jincai Zhang*

Department of Periodontology, Guangdong Provincial Stomatological Hospital, Southern Medical University, Guangzhou, China

ABSTRACT

To investigate whether crosstalk between *RUNX2* and miRNAs is involved in tooth eruption regulated by dental follicle cells (DFCs) and the possible molecular mechanism. Blood samples and embedded dental follicles were collected from patients with cleidocranial dysplasia, and *RUNX2* gene mutations were analyzed, then $RUNX2^{+/m}$ DFCs were isolated and identified. The characteristics of $RUNX2^{+/m}$ DFCs were analyzed. The differential expression of miRNAs was detected between the $RUNX2^{+/m}$ DFCs and $RUNX2^{+/+}$ DFCs by microarray, and target genes were predicted by miRGen. miR-146a was chosen for further investigation, and its effects in DFCs were analyzed by transfecting its mimics and inhibitors, and expression of genes involved in tooth eruption were detected. A novel insertion mutation (c.309_310insTG) of *RUNX2* gene was identified which had an effect on the characteristics of DFCs. Compared with the $RUNX2^{+/+}$ DFCs, there were 69 microRNAs more than twofold up-regulated and 54 microRNAs more than twofold down-regulated in the $RUNX2^{+/m}$ DFCs. Among these, miR-146a decreased significantly in $RUNX2^{+/m}$ DFCs, and expression of *RUNX2*, *CSF-1*, *EGFR*, and *OPG* was significantly altered when miR-146a was overexpressed or inhibited. *RUNX2* gene mutation contributes to the characteristic change of DFCs, and the crosstalk between *RUNX2* gene and miRNAs may be one of the key regulatory mechanisms of differentiation of DFCs. J. Cell. Biochem. 115: 340–348, 2014.

KEY WORDS: CLEIDOCRANIAL DYSPLASIA; *RUNX2* GENE; miRNA

Cleidocranial dysplasia (CCD) is an autosomal dominant hereditary disease characterized by skeletal dysplasia. *RUNX2* (RUNT-related transcription factor 2, Cbfa1) is the master control gene of osteoblast differentiation [Mundlos et al., 1997]. Mutations including missense mutations, deletions, insertions, frameshift and splice mutations in this gene are known to be responsible for CCD. Mutations of the *RUNX2* gene are known to affect the biological behavior of cells [Wise et al., 2002]. The dental follicle is a key player during tooth eruption; however, it remains unknown whether *RUNX2* plays a key role in the differentiation of dental follicle cells (DFCs).

MicroRNAs are non-coding 19–25 nt length small RNAs, which have been reported as powerful post-transcriptional regulators of gene expression, participate in cellular proliferation, cellular differentiation, apoptosis, and various biological processes including growth and disease. However, the influence of miRNAs on DFCs has not been clarified.

There is a crosstalk between transcription factors (TFs) and microRNAs in human protein interaction network [Lin et al., 2012]. It is indicated that the predicted target gene of some microRNAs is *RUNX2* [Huang et al., 2010]. Over-expression of some microRNAs in human mesenchymal stem cells affects the expression of osteoblast/osteoclast and tooth eruption-related genes, inhibits cell proliferation and migration, as well as their osteogenic and adipogenic potential [Tomé et al., 2011].

It is accepted that tooth eruption requires alveolar bone resorption and formation regulated by dental follicle. As the master osteoblast-specific TF, *RUNX2* is essential for osteoblast differentiation; however, whether mutation of *RUNX2* affects expression of miRNAs and plays a role in differentiation of human DFCs (HDFCs) is still

Pei Chen and Dixin Wei have contributed equally.

Grant sponsor: National Natural Science Foundation of China; Grant number: 81271160; Grant sponsor: Medical Scientific Research Foundation of Guangdong Province, China; Grant number: A2012106; Grant sponsor: Nature Science Foundation of Guangdong Province, China; Grant number: S2012010010393.

* Correspondence to: Dongying Xuan and Jincai Zhang, Department of Periodontology, Guangdong Provincial Stomatological Hospital, Southern Medical University, S366 Jiangnan Boulivard, Guangzhou 510280, China.
E-mail: xuanxuan187@126.com; jincaizhang@live.cn

Manuscript Received: 24 April 2013; Manuscript Accepted: 6 September 2013
Accepted manuscript online in Wiley Online Library (wileyonlinelibrary.com): 12 September 2013
DOI 10.1002/jcb.24668 • © 2013 Wiley Periodicals, Inc.

unknown. The HDFCs of embedded teeth are natural human models to study abnormalities of tooth eruption. Therefore, functional analysis of the crosstalk network between *RUNX2* and miRNAs in HDFCs would contribute to uncover the mechanism of tooth eruption.

In the present study, our results suggest that the novel mutation of *RUNX2* gene would affect the characteristics of HDFCs, which may contribute to abnormalities of tooth eruption in patients with CCD, and most importantly, the possible network between *RUNX2* gene and microRNAs might play a key role during the process.

MATERIALS AND METHODS

THE PATIENT WITH CCD AND IDENTIFICATION OF *RUNX2* GENE MUTATION

The patient was a 21-year-old male, who was referred to Guangdong provincial stomatological hospital, complaining of late eruption of permanent dentition and dental abnormalities. Examinations were carried out over the oral cavity and the entire body; the radiological examinations revealed impacted supernumerary teeth, hypoplastic clavicles, delayed closure of the anterior fontanel (Fig. 1), deformity of interphalangeal articulations of the first phalanges joint. According to the diagnostic criteria [Mundlos, 1999], the patient was diagnosed as CCD. His elder sister and their parents with no abnormal symptom were also investigated.

Genomic DNA was extracted from whole blood with the QIAamp Blood Kit (Qiagen, Germany). And the exons 0–7 of *RUNX2* gene was amplified by PCR from genomic DNA, using primers which were reported in the previous study [Xuan et al., 2008]. The PCR reaction was performed with 10× PCR buffer 5 μl, genomic DNA templates 0.5 μl, forward and reverse primer each 0.5 μl, 10 mM dNTP 2 μl, ExTaq polymerase 1 U (Takara, Japan), add H_2O to 50 μl. Reaction conditions: 95°C 5 min; 95°C 40 s, anneal for 40 s, 72°C 40 s, followed by 29 cycles; 72°C 6 min; store at −20°C. PCR sample was purified with Nucleo-trap® PCR Clean-Up Kit (Clontech, Takara, Japan). And DNA sequences were analyzed using BLASTN nucleotide program (http://www.ncbi.nlm.nlh.gov/BLAST).

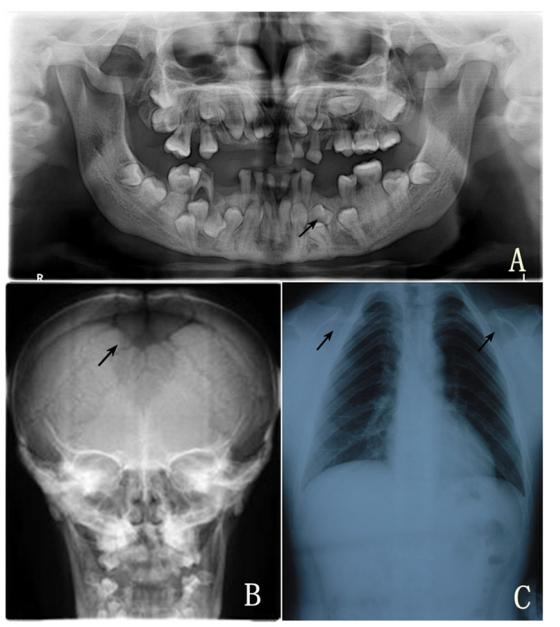

Fig. 1. Radiological morphologies. A: Panoramic radiograph showing impacted supernumerary teeth. B: Posteroanterior cephalometric radiograph showing delayed closure of the anterior fontanel. C: Chest radiograph showing hypoplastic clavicles.

ISOLATION AND CULTURE OF *RUNX2*$^{+/M}$ HDFCs

The *RUNX2*$^{+/m}$ DFCs were isolated and identified from an embedded mandibular premolar (the arrow indicated in Fig. 1) extracted from the patient according to the orthodontic treatment plan. The control *RUNX2*$^{+/+}$ HDFCs was isolated from an embedded tooth extracted from a normal person because of orthodontic treatment, matched in age, gender and tooth position with the CCD patient. Explant culture method was used. DFCs were cultured in Dulbecco′s modified Eagle′s medium (HyClone, USA) with low glucose supplemented with 15%(v/v) fetal bovine serum (FBS; HyClone), 100 U/ml penicillin (HyClone), and 100 μg/ml streptomycin (HyClone) at 37°C in a 5% CO_2 humidified incubator. Non-adherent tissues were removed 3 days later and medium was changed every 3 days. The morphology of HDFCs was observed under microscope. And the mesenchymal natures were identified as vimentin-positive and cytokeratin-negative (mouse monoclonal antibody, Invitrogen, USA) [Hou et al., 1999; Pan et al., 2010]. HDFCs at passage three to five were collected for further experiments. cDNA sequences of HDFCs were analyzed to confirm the mutation of *RUNX2* gene.

Expression of *RUNX2* mRNA and protein were examined by real-time reverse transcription PCR and Western blot. Total RNAs from the cultured DFCs were isolated and reverse transcribed. Primer sequences for *RUNX2* gene were as followed, upstream 5′-GCC ACC GAG ACC AAC AGA GT-3′; downstream 5′-ATT CCG GAG CTC AGC AGA AT-3′, GAPDH was used as control. Reverse transcribed product was amplified with Platinum® Taq DNA polymerase (Invitrogen). Total protein was isolated directly from the cells with the same passage. The protein lysates were resolved by 12% SDS–PAGE, and Western blot analysis was performed using a mouse monoclonal *RUNX2* antibody (ab54868, abcam, 1:500), followed by incubation with a goat peroxidase-tagged anti-mouse IgG secondary antibody. Bands were visualized by ECL reagents.

CHARACTERISTICS OF *RUNX2*$^{+/M}$ HDFCs

The characteristics of the HDFCs were investigated, including morphology, proliferation, and differentiation. Cell area and length of HDFCs were calculated and analyzed using Image-Pro Express version 6.0 software (Olympus Sales & Service Co., Ltd., Guangzhou Branch). Cell proliferation was assessed by CellTiter 96 Cell Proliferation Assay (Promega), and absorbance was measured at 490 nm on a microplate reader (Bio-Rad).

The osteogenic and adipogenic differentiation capacity of HDFCs was assessed. Cells were seeded into 24-well plates. Osteogenic

differentiation was analyzed by culturing cells in osteogenic medium (Sigma) for 21 days, and the degree of mineral nodule formation was estimated using alizarin red S stain. For quantitative analysis, cultures were washed five times with PBS, and mineral was collected after dissolution using 10% (w/v) cetylpyridinium chloride (CPC) in 10 nM sodium phosphate for 15 min at room temperature, then the resulting solutions were measured at 562 nm on a microplate reader (Bio-Rad).

For adipogenic differentiation, HDFCs were induced by OriCell™ Human Mesenchymal Stem Cells Adipogenic Differentiation Medium (Cyagen). After induction 27 days, the cells were examined histologically using 0.3% Oil Red O. For gene-detection, induced HDFCs RNA was extracted using Trizol Reagent (Invitrogen), according to the manufacturer's instruction. PrimeScript RT reagent Kit with gDNA Eraser (Takara, Japan) was used for reverse transcription. And quantitative real-time reverse transcription PCR (qRT-PCR) was performed using SYBR Premix Ex TaqTM II (Takara, Japan). Primer sequences for peroxisome proliferation activator receptor 2 (PPARγ2) and lipoprotein lipase (LPL) are listed in Table I with GAPDH as the internal control.

miRNAs MICROARRAY ANALYSIS

To evaluate the effect of *RUNX2* mutation on miRNAs expression, $RUNX2^{+/m}$ and $RUNX2^{+/+}$ HDFCs were used for miRNA microarray analysis. Total RNA was extracted with Trizol (Invitrogen) from $RUNX2^{+/m}$ and $RUNX2^{+/+}$ HDFCs, respectively, and treated using the mirVana miRNA Isolation Kit (Invitrogen). TaqMan® Array Human MicroRNA A+B Cards Set v3.0 (Applied Biosystems) were used for miRNA expression analysis. Primers used for amplification were Megaplex™ RT Primers (Invitrogen). Evaluation of relative difference of miRNAs was done between $RUNX2^{+/m}$ and $RUNX2^{+/+}$ HDFCs by the comparative cycle threshold. Data analysis was performed using Average Delta Ct protocols [Livak and Schmittgen, 2001; Schmittgen and Livak, 2008].

TARGET GENE PREDICTION

MicroRNAs are known to regulate the expression of genes by binding to the 3′-UTR region of mRNAs. Potential targets of differentially expressed miRNAs were searched using the miRNA target prediction application miRGen [Megraw et al., 2007; Alexiou et al., 2010], which integrates miRNA target prediction and functional analysis of four different prediction databases TargetScan, miRanda, DIANA-microT, and PicTar, and the target genes given by at least three of these databases would be selected. We focused on the genes previously reported to be involved in tooth eruption and osteoblast/osteoclast differentiation, including *RUNX2*, *COX-2*, *MCP-1*, *BMP2*, *OPN*, *ALP*, *OC*, *BSP*, *COL1*, *CAP*, *RANKL*, *CP23*, *CSF-1*, *EGF*, *EGFR*, *IL-1a*, *TNF-a*, *SATB2* [Wise and Fan, 1991; Wise and Lin, 1994; Lin et al., 1996; Shroff et al., 1996; Simonet and Lacey, 1997; Bucay et al., 1998; Mizuno et al., 1998; Que and Wise, 1998; Wise, 1998a, b; Wise et al., 1999]. Gene ontology (GO) function and KEGG pathway enrichments were performed using DAVID bioinformatics resources [Huang et al., 2009].

TABLE I. Primer Sequences Utilized in qRT-PCR

Target gene	Sequence (5′–3′)	Product length (bp)	NCBI no.
RUNX2	F: TGGACGAGGCAAGAGTTTCA R: GGTTCCCGAGGTCCATCTAC	108	NM_004348.3
CSF-1	F: GATTGCAACTGCCTGTACCC R: CAGAGTCCTCCCAGGTCAAG	118	NM_000757.5
OPG	F: GCGCTCGTGTTTCTGGACATC R: CCAGGAGGACATTTGTCACACAAC	119	NM_002546.3
EGFR	F: CACCCTGGTCTGGAAGTACG R: CGGGATCTTAGGCCCATTCG	121	NM_005228.3
PPARγ2	F: CAGAAATGCCTTGCAGTGGG R: ACTCTGGATTCAGCTGGTCG	121	NM_005037.5
LPL	F: GAGGACTTGGAGATGTGGACC R: TTGGAACTGCACCTGTAGGC	118	NM_000237.2

EXPRESSION OF MIR-146A IN $RUNX2^{+/M}$ HDFCs

Among the differently expressed miRNAs, miR-146a was chosen for further experiment, which was 16.96-fold down-regulated in $RUNX2^{+/m}$ HDFCs compared with $RUNX2^{+/+}$ ones and was reported to be related to osteogenic differentiation [Cho et al., 2010].

The miRNA in situ hybridization was performed to confirm the expression of miR-146a in $RUNX2^{+/m}$ and $RUNX2^{+/+}$ HDFCs. Cells were fixed (4% paraformaldehyde) and hybridized with 5′-DIG-labeled miRCURY detection probe (30 nM concentration) (Exiqon, Denmark) specifically targeting miR-146a. Anti-Digoxigenin-AP Fab fragments (Roche, Switzerland) was used for immunologic detection and positive signals were detected using BCIP/NBT color reaction reagent. The cell slides of $RUNX2^{+/m}$ and $RUNX2^{+/+}$ HDFCs were observed and pictured with microscope (Olympus CX41), six visual fields were selected randomly in each group, and the optical density value was measured by Image-Pro Express version 6.0 software (Olympus Sales & Service Co., Ltd., Guangzhou Branch) using the parameter integrated optical density (IOD), the average and variance were calculated.

FUNCTIONAL ANALYSIS OF miR-146a IN HDFCs

$RUNX2^{+/+}$ HDFCs were transfected with miR-146a mimics or inhibitor (5′-FAM labeled) (Invitrogen), respectively, using lipofectamine RNAIMAX reagent (Invitrogen). Twenty-four hours after transfection, HDFCs were digested, and total RNA was extracted, purified using Trizol Reagent (Invitrogen) according to the manufacturer's protocol. PrimeScript RT reagent Kit with gDNA Eraser was used for reverse transcription. And quantitative real-time reverse transcription PCR (qRT-PCR) was performed using SYBR Premix Ex TaqTM II (Takara, Japan) to detect the genes involved in tooth eruption and osteoblast/osteoclast differentiation, such as *RUNX2*, *CSF-1*, *OPG*, and *EGFR*. Primer sequences were listed in Table I. The experiment was repeated three times individually. The evaluation of relative differences was carried out by the Comparative Ct method, using GAPDH as control.

DATA ANALYSIS

Statistical analysis was performed using the statistical software SPSS 13.0. The two comparisons between $RUNX2^{+/m}$ and $RUNX2^{+/+}$ DFCs were performed using two-tailed *t*-test, and the results are expressed as the means ± SE of at least three repeated experiments. A *P*-value 0.05 was considered significant.

RESULTS

IDENTIFICATION OF A NOVEL MUTATION

To identify mutations of the *RUNX2* gene, the genomic DNAs were analyzed from the patient, his healthy sister and parents, and 100 unrelated healthy people. A novel insertion mutation c.309_310insTG was identified in the exon 2 of *RUNX2* gene in the patient (Fig. 2A and B), but not in the healthy families and normal people. The mutation was absent from the SNPs data within the homo sapiens *RUNX2* gene. The insertion was predicted to result in frameshift of the codons, then premature termination code TAG in 144 aa. The same mutation was identified in $RUNX2^{+/m}$ HDFCs.

EFFECT OF *RUNX2* MUTATION ON CHARACTERISTICS OF HDFCs

$RUNX2^{+/m}$ HDFCs express a reduced level of *RUNX2* mRNA (95%, $P > 0.05$) as compared to $RUNX2^{+/+}$ HDFCs (Fig. 2C). The quantitative results (measured by density of bands) demonstrate that the expression of RUNX2 protein in $RUNX2^{+/m}$ HDFCs was decreased to 40% of that in $RUNX2^{+/+}$ HDFCs (Fig. 2D). Compared with $RUNX2^{+/+}$ HDFCs, $RUNX2^{+/m}$ HDFCs had significantly longer and larger morphology (Fig. 3A–D), lower proliferation activity (Fig. 3E and F), and exhibited an increased osteogenic differentiation ability (Fig. 4A and B), moreover, quantitative analysis by cetylpyridinium chloride (CPC) extraction indicated a significant difference ($RUNX2^{+/m}$ HDFCs: 0.962 ± 0.041, $RUNX2^{+/+}$ HDFCs: 0.625 ± 0.037, $P < 0.05$). Compared with $RUNX2^{+/+}$ HDFCs, $RUNX2^{+/m}$ HDFCs exhibited fewer fat droplets after adipogenic induction (Fig. 4C and D). Real-time PCR analysis also exhibited that expression levels of adipocyte-specific PPARγ2 and LPL were significantly lower in $RUNX2^{+/m}$ HDFCs than in $RUNX2^{+/+}$ HDFCs after induction (Fig. 4E), which indicates decreased ability of adipogenic differentiation.

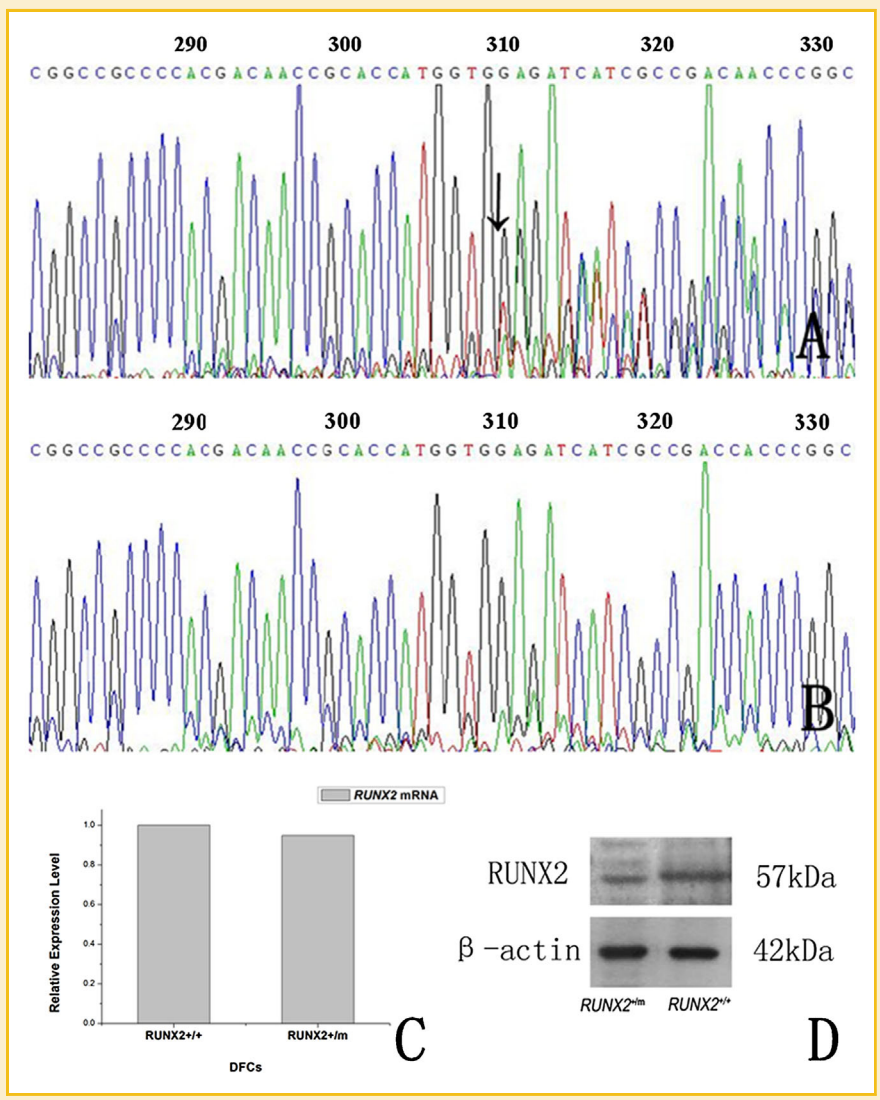

Fig. 2. Mutation analysis of RUNX2 gene in the CCD patient. A: Sequencing results showing the c.309_310insTG mutation. The arrow indicates the mutation site. B: Wild-type sequences. C: *RUNX2* mRNA expression level. D: Western blot results.

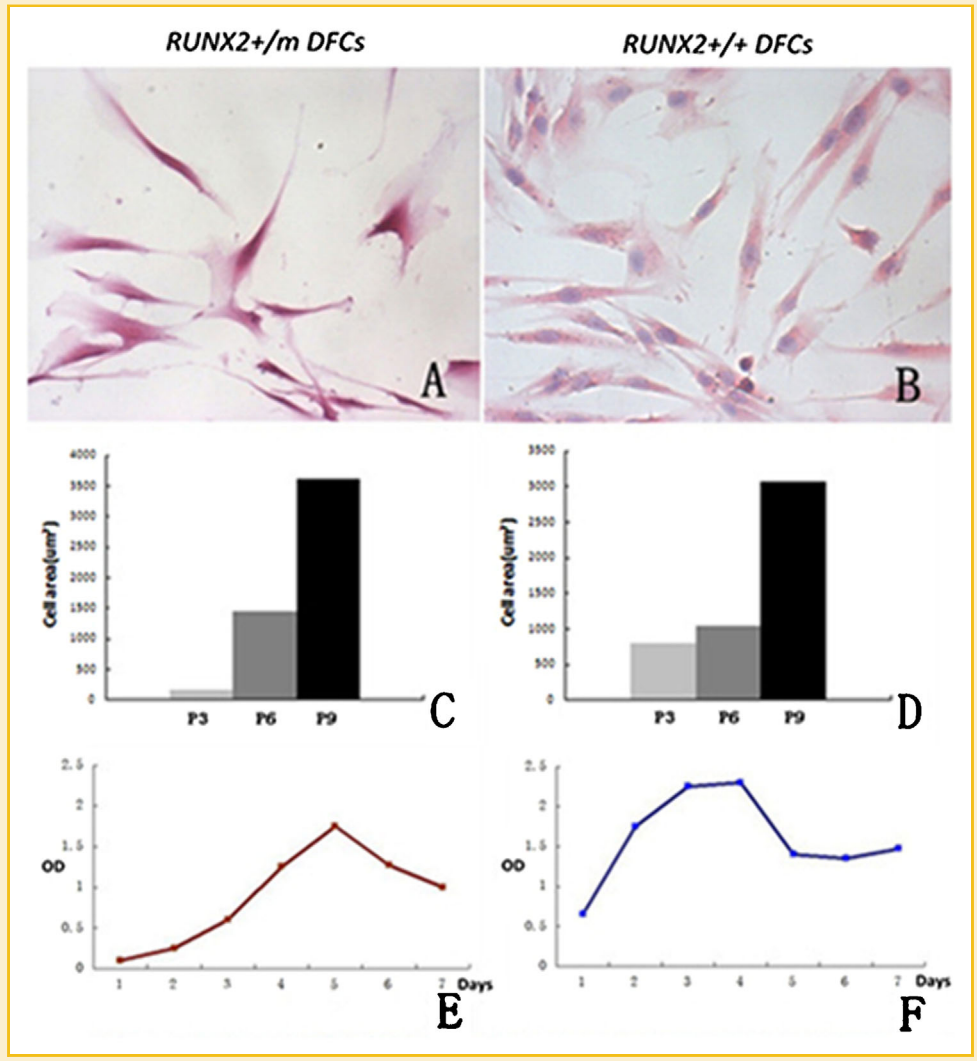

Fig. 3. (A and B) Morphology of HDFCs (HE staining, 400×); (C and D) cell areas of HDFCs; (E and F) HDFCs proliferation at passage 3 (OD of MTS assay).

DIFFERENT EXPRESSION OF miRNAs AND TARGET GENE PREDICTION

miRNA expression profiles were indicated by microarray analysis. Compared with $RUNX2^{+/+}$ HDFCs, there were 69 microRNAs which were more than twofold up-regulated and 54 microRNAs which were more than twofold down-regulated in $RUNX2^{+/m}$ HDFCs.

There were 41 miRNAs with target genes by microRNA target forecast tool analysis. The total number of target genes was 2,718, 8 of which were reported to be related with tooth eruption or osteoblast/osteoclast differentiation (Table II). GO function and KEGG pathway enrichments in DAVID bioinformatics resources were used to analyze functional annotations. The result of GO functions enrichments analysis revealed that the main protein functions of the target genes were related to cellular components and processes and the binding of signals and their receptors.

REGULATION NETWORK BETWEEN *RUNX2* AND miR-146a

miR-146a was chosen for further investigation. It was 16.96-fold down-regulated in microarray analysis, and its expression was confirmed by in situ hybridization (Fig. 5A and B). There was a significant difference in the semi-quantitative analysis (optical density value: $RUNX2^{+/m}$ HDFCs: 27,569.75 ± 10,055.23, $RUNX2^{+/+}$ HDFCs: 47,414.24 ± 17,753.69, $P < 0.05$).

Real-time PCR analysis demonstrated that over-expression of miR-146a may significantly down-regulate the expression of *RUNX2* and *CSF-1* ($P < 0.05$) (Fig. 5C) which was up-regulated when miR-146a was inhibited in transfected HDFCs ($P < 0.05$). Although no significant decrease was found in *OPG* and *EGFR* when miR-146a was overexpressed; OPG and *EGFR* were significantly up-regulated upon miR-146a inhibition ($P < 0.05$).

DISCUSSION

A major manifestation of CCD is facial abnormalities and skeletal dysplasia and is also characterized by impacted supernumerary teeth. In this study, a novel mutation c.309_310insTG of *RUNX2* was identified, and $RUNX2^{+/m}$ HDFCs with the same mutation was successfully isolated. This mutation resulted in frameshift of the code GAG to TGG in 104, then premature termination code in 144, which

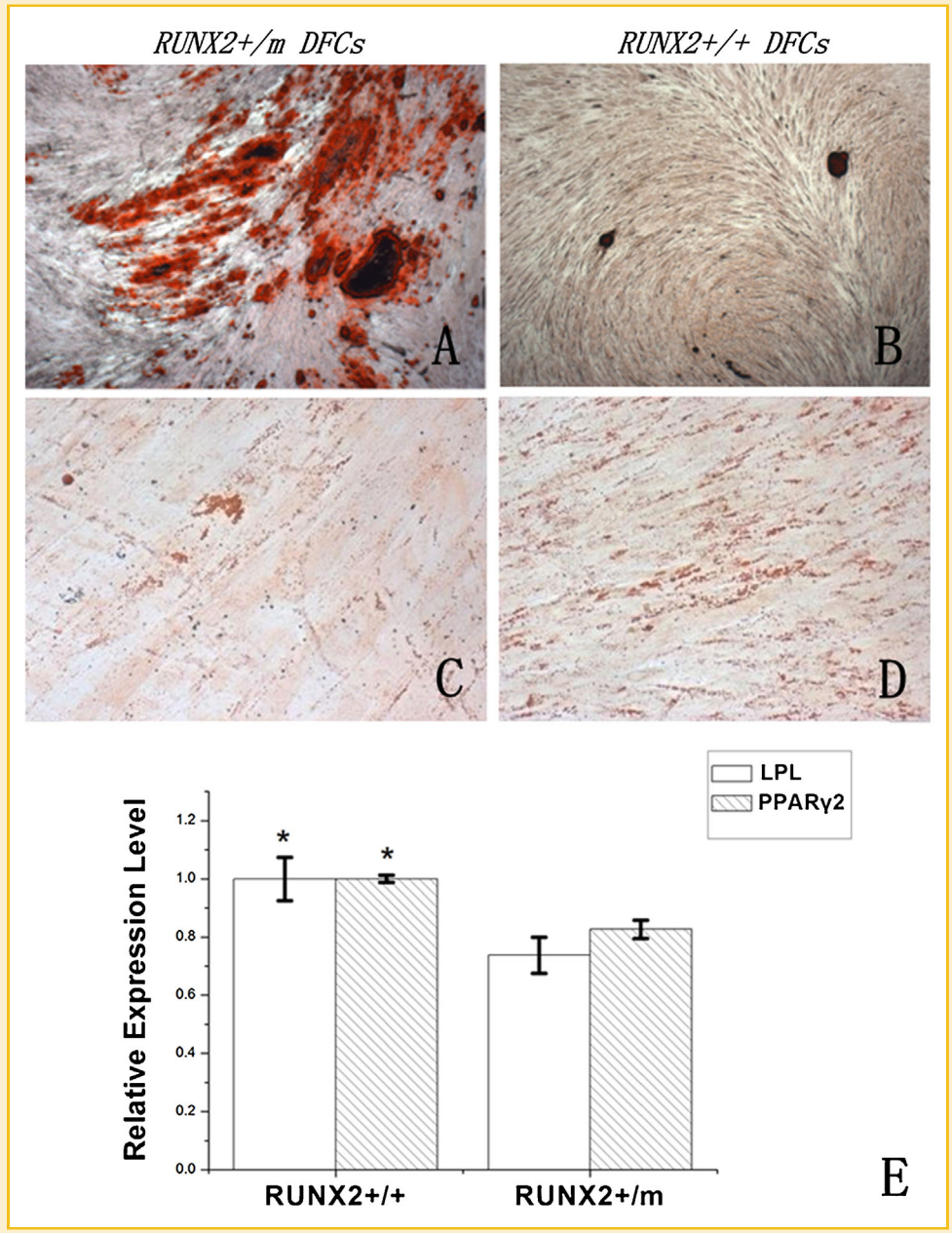

Fig. 4. (A and B) Alizarin red S staining for mineral deposits showed increased osteogenic differentiation ability of *RUNX2*$^{+/m}$ HDFCs (40×); (C and D) oil red O staining for lipid droplets (400×), fewer fat droplets in *RUNX2*$^{+/m}$ HDFCs; (E) Real-time RT-PCR analysis of adipocyte-specific *PPARγ2* and *LPL*.

was predicted to yield amino acids lacking in the C-terminal. Presumably, this mutation was expected to abolish the DNA binding of RUNX2 protein and affect the regulation of genetic expression. Analysis of gene expression demonstrated reduced level of *RUNX2* mRNA and protein in *RUNX2*$^{+/m}$ HDFCs, truncated RUNX2 protein lacking the C-terminal may cause reduction in *RUNX2* biological activities which are related to the biological function of HDFCs.

DFCs, originating from cranial neural crest mesenchyme, have potency of multi-directional differentiation [Pan et al., 2010]. They can differentiate into periodontal ligament, cementum and proper alveolar bone [Bai et al., 2010, 2011; Honda et al., 2011; Jung et al., 2011]. *RUNX2* gene is expressed in dental follicle and regulates tooth eruption. Mutation of *RUNX2* affects the biological behavior of relevant stem cells [Wise et al., 2002]. It has been revealed that *RUNX2* mutation can cause retained deciduous teeth and delayed eruption of permanent teeth. Mutation of *RUNX2* inhibited local osteoclast recruitment and reduced the ability of osteoclasts in *Runx2*$^{+/-}$ mice [Yoda et al., 2004]. Previous research has demonstrated that enamel and dentin of the teeth present insufficient mineralization in patients with CCD, and dental pulp cells (DPCs) with

TABLE II. Target Genes Related to Tooth Eruption

Differential expressed miRNAs	Target genes	Gene function in tooth eruption
miR-204 (4.34-fold down) miR-218 (2.19-fold down) miR-335 (10.72 down) miR-582 (577.69 up)	*RUNX2*	Master transcription factor in osteoblast differentiation
miR-185 (4.29 down) miR-495 (3.86 up) miR-518e (4.18 up) miR-654 (14.53 up)	*BMP2*	Regulating osteoblast/osteoclast differentiation
miR-214 (2.12 down) miR-339 (2.14 down)	*CSF-1*	Formation of passage during tooth eruption
miR-181a (19.06 down) miR-181c (3.88 up) miR-200b (2.17 up)	*IL-1a*	Activate tooth eruption
miR-199a (2.06 down) miR-518b (13.59 up)	*EGF*	Activate tooth eruption
miR-107 (3.97 up) miR-146a (16.96 down) miR-146b (2.11 down) miR-625 (4.13 down)	*TNF-a* *EGFR*	Recruitment of monocytes in dental follicle, promote osteoblast differentiation Strong positive in early stage of dental follicle
miR-107 (3.97 up) miR-204 (4.34 down) miR-218 (2.19 down) miR-23b (4.33 down) miR-31 (3.81 up) miR-320 (2.10 down) miR-335 (10.72 down) miR-339 (2.14 up) miR-424 (2.18 up) miR-495 (3.86 up) miR-655 (3.89 up) miR-93 (2.18 down)	*SATB2*	Cooperation with *RUNX2*, enhance the regulation of osteoblasts differentiation

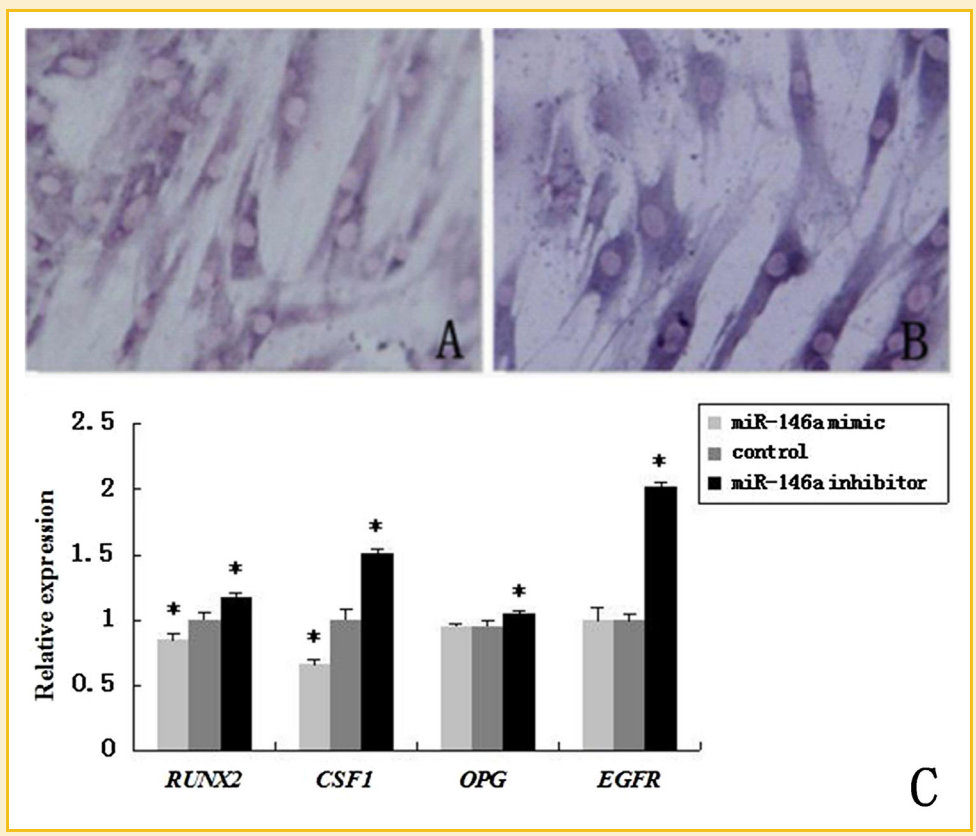

Fig. 5. In situ hybridization results showed that expression of miR-146a decreased in $RUNX2^{+/m}$ HDFCs (A) compared with $RUNX2^{+/+}$ HDFCs (B) (400×). C: Real-time PCR analysis of *RUNX2*, *CSF-1*, *OPG*, *EGFR* mRNA expression after miR-146a mimic/inhibitor transfection. Compared with control, $^{*}P < 0.05$.

RUNX2 mutation present a lower rate of proliferation, and weaker ability of calcification [Xuan et al., 2010].

Tooth eruption is a complex process regulated by osteoblasts and osteoclasts interaction and affected by various factors. The mechanism has not yet been well clarified. It is known that dental follicle is necessary for tooth eruption. One of the symptoms of CCD is delayed eruption of permanent teeth; therefore, the DFCs of unerupted teeth serve as natural human models to study eruption abnormalities.

Recent surveys demonstrate that miRNAs affect *RUNX2* or other bone-related gene expression, thereby up or down-regulate osteogenic differentiation. In vivo silencing of miR-2861 in mice reduced RUNX2 protein expression and inhibited bone formation [Li et al., 2009]. miR-204/211 act as important endogenous negative regulators of *RUNX2*, which inhibit osteogenesis of BMSCs [Huang et al., 2010]. TFs and miRNAs are both gene regulators. It was revealed that there is crosstalk between TF and miRNAs in the human protein interaction network [Lin et al., 2012]. The TF appears to regulate the miRNAs, or to be regulated by the miRNAs, forming a diversity of feed-forward loops [Shalgi et al., 2007]. As the master osteoblast-specific TF, the mutation of RUNX2 gene may affect miRNAs expression.

In this study, the TaqMan® Array Human MicroRNA A+B Cards were used to detect differentially expressed miRNAs between $RUNX2^{+/m}$ and $RUNX2^{+/+}$ HDFCs. There were 69 miRNAs up-regulated and 54 miRNAs down-regulated in the DFCs with the RUNX2 mutation. Among the target genes, *BMP2* was a target of several differentially expressed miRNAs, and it was reported to induce the undifferentiated mesenchymal progenitors to differentiate into osteoblasts [Yamaguchi, 1995]. The *TGF-beta* superfamily played many important roles in the differentiation process of the skeletal mesenchymal cells [Yamaguchi, 1995]. Wnt pathway regulation by demineralized bone was approximated by both *BMP-2* and *TGF*-β signaling [Zhou et al., 2013]. Therefore, *TGF*-β/*BMP* pathway was predicted to be involved in tooth eruption. However, in our KEGG pathway enrichments results, *TGF*-β/*BMP* pathway was not in the top 5, so it was not further investigated. It was referred that the altered expression of miRNAs and target genes may contribute to change of differentiation of HDFCs, which may be one of the mechanisms of delayed tooth eruption.

miR-146a can regulate innate immune and inflammatory response [Li et al., 2010; Roy and Sen, 2011], and may function as a potent tumor suppressor [Paik et al., 2011]. Over-expression of miR-146a induced the inhibition of IRAK1 expression and inhibited osteogenic differentiation [Cho et al., 2010]. In the study, miR-146a was 16.96-fold down-regulated, which is predicted to target EGFR, a gene related to tooth eruption. Upon over-expression of miR-146a, there were significant differences in the relative expression level of *RUNX2* and *CSF-1* among three groups (miR-146a mimic, control, and miR-146a inhibitor, $P < 0.05$). For *OPG* and *EGFR* expression, there was no significant difference after miR-146a mimic transfection ($P > 0.05$), but significant difference was found between control and miR-146a inhibitor transfected HDFCs ($P < 0.05$). *EGFR*-mediated signaling pathway has been shown to participate in many developmental processes and plays a role in anabolic metabolism of bone [Zhang et al., 2011]. *EGFR* signaling increases the protein amounts of transcription corepressor *HDAC4*, which regulates *RUNX2* expression in differentiating osteoblasts [Zhu et al., 2011]. Since *EGFR* is one of the target genes of miR-146a, there may be a complicated regulation network between *EGFR*, *RUNX2*, and miR-146a.

In conclusion, a novel mutation of *RUNX2* was identified, which affected miRNAs expression, and may contribute to the change of HDFCs characteristics and may have potential impact on tooth eruption. This is the first time that we have found the differential expressed miRNAs between human DFCs with or without *RUNX2* mutation. Further functional analysis of the *RUNX2* and miRNA regulatory network is needed to clarify the mechanism, which may provide new insights into the understanding of dental eruption abnormalities in CCD patients.

ACKNOWLEDGMENTS

We are grateful to Matt Devine for proof reading the manuscript. We thank the patient and his families for their cooperation and enthusiastic support.

REFERENCES

Alexiou P, Vergoulis T, Gleditzsch M, Prekas G, Dalamagas T, Megraw M, Grosse I, Sellis T, Hatzigeorgiou AG. 2010. miRGen 2.0: A database of microRNA genomic information and regulation. Nucleic Acids Res 38 (databaseissue):D137–D141.

Bai Y, Bai Y, Matsuzaka K, Hashimoto S, Kokubu E, Wang X, Inoue T. 2010. Formation of bone-like tissue by dental follicle cells co-cultured with dental papilla cells. Cell Tissue Res 342(2):221–231.

Bai Y, Bai Y, Matsuzaka K, Hashimoto S, Fukuyama T, Wu L, Miwa T, Liu X, Wang X, Inoue T. 2011. Cementum and periodontal ligament-like tissue formation by dental follicle cell sheets co-cultured with Hertwig's epithelial root sheath cells. Bone 48(6):1417–1426.

Bucay N, Sarosi I, Dunstan CR. 1998. Osteoprotegerin-deficient mice develop early onset osteoporosis and arterial calcification. Genes Dev 12(9):1260–1268.

Cho HH, Shin KK, Kim YJ, Song JS, Kim JM, Bae YC, Kim CD, Jung JS. 2010. NF-kappaB activation stimulates osteogenic differentiation of mesenchymal stem cells derived from human adipose tissue by increasing TAZ expression. J Cell Physiol 223(1):168–177.

Honda MJ, Imaizumi M, Suzuki H, Ohshima S, Tsuchiya S, Satomura K. 2011. Stem cells isolated from human dental follicles have osteogenic potential. Oral Surg Oral Med Oral Pathol Oral Radiol Endod 111(6):700–708.

Hou LT, Liu CM, Chen YJ, Wong MY, Chen KC, Chen J, Thomas HF. 1999. Characterization of dental follicle cells in developing mouse molar. Arch Oral Biol 44(9):759–770.

Huang da W, Sherman BT, Lempicki RA. 2009. Systematic and integrative analysis of large gene lists using DAVID bioinformatics resources. Nat Protoc 4 (1):44–57.

Huang J, Zhao L, Xing L, Chen D. 2010. MicroRNA-204 regulates Runx2 protein expression and mesenchymal progenitor cell differentiation. Stem Cells 28(2):357–364.

Jung HS, Lee DS, Lee JH, Park SJ, Lee G, Seo BM, Ko JS, Park JC. 2011. Directing the differentiation of human dental follicle cells into cementoblasts and/or osteoblasts by a combination of HERS and pulp cells. J Mol Histol 42 (3):227–235.

Li H, Xie H, Liu W, Hu R, Huang B, Tan YF, Xu K, Sheng ZF, Zhou HD, Wu XP, Luo XH. 2009. A novel microRNA targeting HDAC5 regulates osteoblast differentiation in mice and contributes to primary osteoporosis in humans. J Clin Invest 119(12):3666–3677.

Li L, Chen XP, Li YJ. 2010. MicroRNA-146a and human disease. Scand J Immunol 71(4):227–231.

Lin F, Zhao L, Wise GE. 1996. In vivo acid in vitro effects of epidermal growth factor on its receptor gene expression in rat dental follicle cells. Arch Oral Biol 41(5):485–491.

Lin CC, Chen YJ, Chen CY, Oyang YJ, Juan HF, Huang HC. 2012. Crosstalk between transcription factors and microRNAs in human protein interaction network. BMC Syst Biol 6:18.

Livak KJ, Schmittgen TD. 2001. Analysis of relative gene expression data using real-time quantitative PCR and the 2(-Delta Delta Ct) Method. Methods 25 (4):402–408.

Megraw M, Sethupathy P, Corda B, Hatzigeorgiou AG. 2007. miRGen: A database for the study of animal microRNA genomic organization and function. Nucleic Acids Res 35(databaseissue):D149–D155.

Mizuno A, Amizuka N, Irie K. 1998. Severe osteoporosis in mice lacking osteoclastogenesis inhibitory factor/osteoprotegerin. Biochem Biophys Res Commun 247(3):610–615.

Mundlos S., Cleidocranial dysplasia: Clinical and molecular genetics. J Med Genet 1999;36(3):177–182.

Mundlos S, Otto F, Mundlos C, Mulliken JB, Aylsworth AS, Albright S, Lindhout D, Cole WG, Henn W, Knoll JH, Owen MJ, Mertelsmann R, Zabel BU, Olsen BR. 1997. Mutation involving the transcription factor CBFA1 cause cleidocranial dysplasia. Cell 89(5):773–779.

Paik JH, Jang JY, Jeon YK, Kim WY, Kim TM, Heo DS, Kim CW. 2011. MicroRNA-146a downregulates NFκB activity via targeting TRAF6 and functions as a tumor suppressor having strong prognostic implications in NK/T cell lymphoma. Clin Cancer Res 17(14):4761–4771.

Pan K, Sun Q, Zhang J, Ge S, Li S, Zhao Y, Yang P. 2010. Multilineage differentiation of dental follicle cells and the roles of Runx2 over-expression in enhancing osteoblast/cementoblast-related gene expression in dental follicle cells. Cell Prolif 43(3):219–228.

Que BG, Wise GE. 1998. Tooth eruption molecules enhance MCP-L gene expression in the dental follicle of the rat. Dev Dyn 212(3):346–351.

Roy S, Sen CK. 2011. miRNA in innate immune responses: Novel players in wound inflammation. Physiol Genomics 43(10):557–565.

Schmittgen TD, Livak KJ. 2008. Analyzing real-time PCR data by the comparative Ct method. Nat Protoc 3(6):1101–1108.

Shalgi R, Lieber D, Oren M, Pilpel Y. 2007. Global and local architecture of the mammalian microRNA–Transcription factor regulatory network. PLoS Comput Biol 3(7):e131.

Shroff B, Kashner JE, Norris K. 1996. Epidermal growth factor and epidermal growth factor-receptor expression in the mouse dental follicle during tooth eruption. Arch Oral Biol 41(6):613–617.

Simonet WS, Lacey DL. 1997. Osteoprotegerin: A novel secreted protein involved in the regulation of bone density. Cell 89(2):309–319.

Tomé M, López-Romero P, Albo C, Sepúlveda JC, Fernández-Gutiérrez B, Dopazo A, Bernad A, González MA. 2011. miR-335 orchestrates cell proliferation, migration and differentiation in human mesenchymal stem cells. Cell Death Differ 18(6):985–995.

Wise GE. 1998a. In vivo effect of interleukin-1a on colony-stimulating factor-1 gene expression in the dental follicle of the rat molar. Arch Oral Biol 43 (2):163–165.

Wise GE. 1998b. Effect of CSF-1 an in vivo expression of c-fos in the dental follicle during tooth eruption. Eur J Oral Sci 106(Suppl1):397–400.

Wise GE, Fan W. 1991. Immunolocalization of transforming growth factor beta in rat molars. J Oral Pathol Med 20(2):74–80.

Wise GE, Lin F. 1994. Regulation and localization of colony-stimulating factor-1 mRNA in cultures rat dental follicle cells. Arch Oral Biol 39(7):521–627.

Wise GE, Que BG, Huang H. 1999. Synthesis and secretion of MCP-1 by dental follicle cells-implications for tooth eruption. J Dent Res 78(l):1677–1681.

Wise GE, Frazier-Bowers S, D′Souza RN. 2002. Cellular, molecular, and genetic determinants of tooth eruption. Crit Rev Oral Biol Med 13(4):323–334.

Xuan D, Li S, Zhang X, Hu F, Lin L, Wang C, Zhang J. 2008. Mutations in the RUNX2 gene in Chinese patients with cleidocranial dysplasia. Ann Clin Lab Sci 38(1):15–24.

Xuan D, Sun X, Yan Y, Xie B, Xu P, Zhang J. 2010. Effect of cleidocranial dysplasia-related novel mutation of RUNX2 on characteristics of dental pulp cells and tooth development. J Cell Biochem 111(6):1473–1481.

Yamaguchi A. 1995. Regulation of differentiation pathway of skeletal mesenchymal cells in cell lines by transforming growth factor-beta superfamily. Semin Cell Biol 6(3):165–173.

Yoda S, Suda N, Kitahara Y, Komori T, Ohyama K. Zhang X. 2004. Delayed tooth eruption and suppressed osteoclast number in the eruption pathway of heterozygous Runx2/Cbfal knockout mice. Arch Oral Biol 49(6):435–442.

Zhang X, Tamasi J, Lu X, Zhu J, Chen H, Tian X, Lee TC, Threadgill DW, Kream BE, Kang Y, Partridge NC, Qin L. 2011. Epidermal growth factor receptor plays an anabolic role in bone metabolism in vivo. J Bone Miner Res 26(5):1022–1034.

Zhou S, Mizuno S, Glowacki J. 2013. Wnt pathway regulation by demineralized bone is approximated by both BMP-2 and TGF-β1 signaling. J Orthop Res 31(4):554–560.

Zhu J, Shimizu E, Zhang X, Partridge NC, Qin L. 2011. EGFR signaling suppresses osteoblast differentiation and inhibits expression of master-osteoblastic transcription factors Runx2 and Osterix. J Cell Biochem 112(7): 1749–1760.